Mechanisms underlying the resistance of human papillomavirus-infected or -transformed cells to Th1 immunity

Ma, W.

Chapter 2

Human papillomavirus downregulates the expression of IFITM1 and RIPK3 to escape from IFNγ-and TNFα-mediated anti-proliferative effects and necroptosis

Ma W, Tummers B, Van Esch EM, Goedemans R, Melief CJ, Meyers C, Boer JM, Van Der Burg SH.

Front Immunol. 2016 Nov 22;7:496

Human papillomavirus (HPV) downregulates the expression of IFITM1 and RIPK3 to escape from IFNγ and TNFα-mediated anti-proliferative effects and necroptosis

Wenbo Ma[1*], Bart Tummers[1*], Edith M.G. van Esch[2], Renske Goedemans[1], Cornelis J.M. Melief[3], Craig Meyers[4], Judith M. Boer[5], Sjoerd H. van der Burg[1,§].

[1]Department of Clinical Oncology, Leiden University Medical Center, Leiden, The Netherlands.
[2]Department of Gynaecology, Leiden University Medical Center, Leiden, The Netherlands.
[3]Department of Immunohematology and Blood Transfusion, Leiden University Medical Center, Leiden, The Netherlands.
[4]Department of Microbiology and Immunology, The Pennsylvania State University College of Medicine, Hershey, USA
[5]Human Genetics, Leiden University Medical Center, Leiden, The Netherlands; Current address: Department of Pediatric Oncology, Erasmus MC - Sophia Children's Hospital, Rotterdam, The Netherlands and Netherlands Bioinformatics Center, Nijmegen, The Netherlands

* Both authors contributed equally

[§]Corresponding author: Prof. Dr. S.H. van der Burg, Dept. of Clinical Oncology, Building 1, K1-P, Leiden University Medical Center, PO box 9600, 2300 RC Leiden, The Netherlands. Phone: +31-71-5261180, Fax: +31-71-5266760, E-mail: shvdburg@lumc.nl

Key words
HPV, infection, immune escape, Th1 cytokines.

Abstract
The clearance of a high-risk human papillomavirus (hrHPV) infection takes time and requires the local presence of a strong type 1 cytokine T cell response, suggesting that hrHPV has evolved mechanisms to resist this immune attack. Using an unique system for non, newly and persistent hrHPV infection, we show that hrHPV infection renders

keratinocytes (KCs) resistant to the anti-proliferative and necroptosis inducing effects of IFNγ and TNFα. HrHPV-impaired necroptosis was associated with the upregulation of several methyltransferases, including EZH2 and the downregulation of RIPK3 expression. Restoration of RIPK3 expression using the global histone methyltransferase inhibitor 3-deazaneplanocin increased necroptosis in hrHPV-positive KCs. Simultaneously, hrHPV effectively inhibited IFNγ/TNFα-mediated arrest of cell growth at the S-phase by downregulating *IFITM1* already at 48 hours after hrHPV infection, followed by an impaired increase in the expression of the anti-proliferative gene *RARRES1* and a decrease of the proliferative gene *PCNA*. Knockdown of *IFITM1* in uninfected KCs confirmed its role on *RARRES1* and its anti-proliferative effects. Thus, our study reveals how hrHPV deregulates two pathways involved in cell death and growth regulation to withstand immune mediated control of hrHPV-infected cells.

Introduction

High-risk human papillomaviruses (hrHPVs) infect undifferentiated keratinocytes (KCs) of squamous epithelia. Persistent infections may lead to cancers of the anogenital region as well as of the head and neck [1]. In order to establish a persistent and productive infection, hrHPV requires access to the undifferentiated KCs that make up the epithelial basal layer and have the capacity to divide [2]. High-risk HPV infections can persist despite viral activity in keratinocytes, indicating that HPV has developed mechanisms to evade or suppress the innate and/or adaptive immune response of the host. Indeed, hrHPV utilizes its viral proteins and exploits cellular proteins to interfere with signaling of innate immune pathways, potentially postponing the activation of an adaptive immune response [3]. HPV may attenuate immune signaling at different levels in the STAT [4-7], IRF and NFκB pathways [8-14], and has also been shown to impair IFNγ and TNFα signaling [15]. Nevertheless, T cells will become activated and migrate to infected sites. Studies in healthy individuals, immunosuppressed patients and in patients with spontaneously or vaccine-induced

regressions revealed an important role for a strong type 1 (IFNγ and TNFα)-associated HPV early antigen-specific T cell response in the control of HPV infected lesions [16]. However, even vaccines that boost viral Th1 immunity during chronic infection are only partially successful [17-19] with a positive clinical outcome only in patients with a very strong Th1 response [18, 20], suggesting that hrHPV may have found ways to resist the effector cytokines of the adaptive immune system.

IFNγ is a pleiotropic cytokine that affects immune regulation, immune surveillance, inflammation, tumor suppression, and has antiviral as well as anti-proliferative properties. Binding of IFNγ to the IFNγ receptor (IFNγR) leads to JAK1/2-mediated STAT1 phosphorylation, dimerization and nuclear translocation that results in interferon-stimulated gene (ISG)-expression [21]. IFNγ may also induce necroptotic cell death by the JAK1/STAT1-dependent activation of proteins, encoded by interferon stimulated genes, that drive various aspects of the RIPK1–RIPK3 necrosome complex assembly [22], including the RNA-responsive protein kinase PKR which then interacts with RIPK1 to trigger necroptosis [23]. TNFα also regulates cell survival, apoptosis or necroptosis via an intricate network of signals that operate downstream of TNF receptor 1 (TNFR1). Binding of TNF to TNFR1 leads to NFκB activation through cIAP-mediated ubiquitylation of RIPK1. Under circumstances that RIPK1 is deubiquitylated it can associate with FADD to recruit and homodimerize caspase-8 leading to the induction of apoptosis. RIPK1 can also bind and activate RIPK3 after which MLKL is activated and necroptosis ensues. $cFLIP_L$ is expressed upon NFκB signaling (as *CFLAR*), heterodimerizes with caspase-8 on FADD and as such prevents apoptosis by abrogating full caspase-8 activation and necroptosis by disrupting the interaction between RIPK1 and RIPK3. [24].
IFNγ and TNFα are known to synergize in the suppression of KC proliferation [25]. IFNγ induces growth arrest and differentiation [26, 27]. TNFα also induces growth arrest but there are conflicting data concerning its capacity to induce cell death of primary KCs [25, 28].

Exposure of KCs to both IFNγ and TNFα potently stimulates the production of nitric oxide synthase (iNOS) to induce the upregulation of FasL, Fas receptor activation and subsequent caspase-mediated apoptosis of KCs [29], an effect to which differentiated KCs are especially sensitive [30]. However, the ability of HPV-infected undifferentiated KCs to resist the effects of IFNγ and/or TNFα on proliferation as well as the underlying mechanisms are not well understood. In this study, we evaluated the influence of hrHPV on the IFNγ and TNFα-mediated cell growth inhibition and cell death induction of undifferentiated KCs by functional and biochemical assays. We utilized a system that resembles the natural infection with HPV as closely as possible, comprising of primary KCs that stably maintain the hrHPV genome as episomes and were shown to undergo the entire differentiation-dependent HPV life cycle in organotypic raft cultures, non-infected primary KC cultures and primary KCs newly infected with authentic HPV16 virions (Karim et al., 2013), to show that hrHPV presence renders KCs more resistant to both necroptosis and the anti-proliferative effects instigated by IFNγ and TNFα, and reveal the biological mechanisms responsible.

Material and Methods

Ethics statement

The use of discarded human foreskin, cervical and vaginal KC tissues to develop cell lines for these studies was approved by the institutional review board at the Pennsylvania State University College of Medicine and by the institutional review board at Pinnacle Health Hospitals. The Medical Ethical Committee of the Leiden University Medical Center approved the human tissue sections (healthy foreskin, healthy cervix and HPV16- or 18-positive cervical neoplasia) used for staining. All sections and cell lines were derived from discarded tissues and de-identified, therefore no informed consent was necessary.

Cell culture

Primary cultures of human epithelial keratinocytes (KCs) were established from foreskin, vaginal, vulva and cervical tissues as previously described [31] and grown in keratinocyte serum-free medium (EpiLife® Medium, with 60 µM calcium supplemented with HKGS kit, Invitrogen, Breda, The Netherlands). KCs stably maintaining the full episomal HPV genome following electroporation (HPV-positive KCs) were grown in monolayer culture using E medium in the presence of mitomycin C (Sigma-Aldrich) treated J2 3T3 feeder cells [32, 33] for two passages and were then adapted to EpiLife® Medium for one passage before experimentation. J2 3T3 mouse fibroblasts were cultured in Iscove's modified Dulbecco's medium supplemented with 8% fetal bovine serum, 2 mM l-glutamine and 1% penicillin-streptomycin (complete IMDM medium) (Gibco-BRL, Invitrogen).

Reagents

Recombinant human TNFα (Rhtnf-a, Invivogen/bioconnect, France), Recombinant Human Interferonγ (11343536, Immunotools, Germany), BV-6 (S7597, Selleckchem, Netherlands), Pan Caspase Inhibitor Z-VAD-FMK (FMK001, R&Dsystems, USA), 3-Deazaneplanocin A (DZNep) hydrochloride (A8182, Apexbt, Netherlands), Nec-1s (2263-1, Biovision, California, USA), Cycloheximide (CHX) solution (C4859, SIGMA, Netherlands), GSK503 (S7804, Selleckchem, Netherlands).

Analysis of IFNGR1, TNFR1 and TNFR2 cell surface expression

The expression of the receptors for the cytokines IFNγ and TNFα was analyzed by flow cytometry after staining of the cells with the antibodies (1:10 diluted) against IFNGRα (Mouse anti-human CD119-PE, clone GIR-94, BD Biosciences, Breda, the Netherlands), TNFR1 (mouse anti-human CD120a-PE, clone 16803, R&D systems, Abingdon, UK) or TNFR2 (mouse anti-human CD120b-PE, clone MR2.1, Invitrogen Life Technologies, Bleiswijk, the Netherlands). Briefly, cells were transferred into wells of V-bottom 96-wells plate, washed with ice-cold PBS+0.5% BSA and incubated for 10 minutes on ice with ice-cold PBS (B.Braun, Melsungen, Germany)+0.5% Bovine Serum Albumin (Sigma Aldrich) +10% Fetal Calf Serum(PAA Laboratories, Lelystad, the Netherlands). Then, the cells were washed again and

incubated for 30 minutes on ice in the dark with the antibody indicated. Following one wash step the cells were fixed in 1% paraformaldehyde before they were acquired by BD Fortessa with BD FACSDiv software version 6.2, and data analyzed using FlowJo version 10.0.7 (Treestar, Olten, Switzerland).

HPV16 knock-down in HPV16-positive KCs and infection of undifferentiated keratinocytes

HPV16-positive KCs were transfected with 50 nM Control or HPV16 E2 siRNA as previously described [13]. Primary basal layer human foreskin keratinocytes were infected with native HPV16 at MOI 100 as previously described [13]. Cells were washed and harvested and target gene expression was assayed by RT-qPCR.

IFITM1 knock-down in undifferentiated KCs

shRNA's were obtained from the MISSION TRC-library of Sigma-Aldrich (Zwijndrecht, The Netherlands). The MISSION shRNA clones are sequence-verified shRNA lentiviral plasmids (pLKO.1-puro) provided as frozen bacterial glycerol stocks (Luria Broth, carbenicillin at 100 µg/ml and 10% glycerol) in E. coli for propagation and downstream purification of the shRNA clones. pLKO.1 contains the puromycin selection marker for transient or stable transfection. The construct against IFITM1 (NM_003641) was TRCN0000057499: CCGGCCTCATGACCATTGGATTCATCTCGAGATGAATCCAATGGTCATGA GGTTTTTG and the control was: SHC004 (MISSION TRC2-pLKO puro TurboGFP shRNA Control vector):CCGGCGTGATCTTCACCGACAAGATCTCGAGATCTTGTCGGTGAA GATCACGT TTTT. KCs at ~60% confluency were transduced with lentivirus at MOI 5-10 over night, after which medium was replaced. At least 72 hours post-transduction cells were harvested, washed and plated as indicated and allowed to attach overnight. Cell were stimulated as indicated and assayed accordingly.

RNA expression analyses

The micro array data [14] is accessible in the Gene Expression Omnibus database (accession number GSE54181). Plots were

generated using the webtool R2: microarray analysis and visualization platform (http://r2.amc.nl).
Total RNA was isolated using the NucleoSpin RNA II kit (Machery-Nagel, Leiden, The Netherlands) according to the manufacturer's instructions. Total RNA (0.5 – 1.0 µg) was reverse transcribed using the SuperScript III First Strand synthesis system from Invitrogen. TaqMan PCR was performed using TaqMan Universal PCR Master Mix and pre-designed, pre-optimized primers and probe mix for IFITM1, GLB1, BCL-2, Bax, RARRES1, PCNA and GAPDH (Applied Biosystems, Foster City, USA). Threshold cycle numbers (Ct) were determined using the CFX PCR System (BioRad, Veenendaal, The Netherlands) and the relative quantities of cDNA per sample were calculated using the ΔΔCt method using GAPDH as the calibrator gene.

Western blot analysis

Polypeptides were resolved by SDS–polyacrylamide gel electrophoresis (SDS–PAGE) and transferred to a nitrocellulose membrane (Bio-Rad, Veenendaal, The Netherlands). Immunodetection was achieved with primary antibodies against TRAF2 (#4724s, Cell Signaling Technology (CST), Leiden, Netherlands), cIAP1 (#7065p, CST), cIAP2 (#3130s,CST), XIAP (#14334, CST), RIPK1 (#3493, CST), cFLIP (#3210, CST), caspase-8 (#9746, CST), cleaved caspase-8 (#9496s, CST), FADD (#2782, CST), RIPK3 (#13526, CST), MLKL (#14993s, CST), phospho-MLKL (phospho S358; ab187091, Abcam, Cambridge, UK), EZH2 (612667, BD Biosciences, The Netherlands), IFITM1 (PA5-20989, Thermo Scientific, Netherlands), Trimethyl-Histone H3 (Lys27)(07-449, Merk Millipore), STAT1 (#9172, CST), phospho-STAT1 (Tyr701, #9167, CST), β-actin (A5316, Sigma-Aldrich, Germany), and HRP-coupled anti-mouse (#7076s, CST) and HRP-coupled anti-rabbit (#7074s, CST) secondary antibodies. Chemoluminescence reagent (#170-5060, Bio-Rad, Germany) was used as substrate and signal was scanned using the Chemidoc and accompanying Software (Image Lab Software Version 5.2.1, Bio-Rad).

Proliferation assay

KCs, hrHPV+KCs, control shRNA-expressing KCs, or IFITM1 shRNA-expressing KCs were seeded 5000 cell/well in 96-well plates and allowed to attach overnight. Cells were cultured in presence of indicated concentrations of IFNγ and/or TNFα in 150 µl for 96 hours. 15 µl/well MTT (3-(4,5-dimethylthiazol-2-yl)-2,3-diphenyl-2*H*-tetrazolum bromide) stock solution (5 mg/ml in 0.1 M PBS) was added for 3 hours. When the purple formazan precipitate was clearly visible under the microscope, bright light pictures were made using an Olympus IX51 inverse fluorescence microscope (Olympus, Zoeterwoude, The Netherlands). Images were captured by ColorView II Peltier-cooled charge-coupled device camera (Olympus) and archived using Cell^F software (Olympus).

Cellular DNA content analysis.

The CyQuant-NF assay (C35006, ThermoFisher Scientific, USA), which measures cellular DNA content via fluorescent dye binding, was used to quantify the cell number in cultures treated with increasing doses of IFNγ. Briefly, control shRNA-expressing KCs, or IFITM1 shRNA-expressing KCs were seeded 500 cell/well in 96-well plates and allowed to attach overnight. Cells were cultured in presence of indicated concentrations of IFNγ, in triplicate wells, for 96 hours and then processed according to the protocol for adherent cells provided by the manufacturer. The fluorescence intensity detected is a measure for the number of cells present in the wells.[34]

Cell cycle analysis of keratinocytes

Following the treatment of KCs with 250 IU/ml IFNγ for 48 hours, the cells were fixed in 70% ethanol at 4˚C overnight. The fixed cells were washed with cold PBS and subsequently incubated for 30 minutes with 10 µg/ml RNase (#R6513, Sigma-aldrich) and 10 µg/ml propidium iodide (P4170, Sigma-Aldrich) staining. Cell cycle was detected by flow cytometry (BD Accuri™ C6, BD biosciences, The Netherlands) and analyzed using FlowJo v10.0.8.

SYTOX green dead cell assay

Replicate cultures of cells were plated in 6-wells tissue culture plates. Following the indicated treatments, all adhering and floating cells were collected with TrypLE™ Express Enzyme (12604-021, Thermofisher). The cells were washed with HBSS (14025-092, Thermofisher) once and then incubated with 5 µM SYTOX® Green Nucleic Acid Stain (S7020, Thermofisher) in absence or presence of 1µg/ml DAPI (D9542, Sigma Aldrich) at 20°C for 30 min. The cells were washed with HBSS and mixed with VECTASHIELD Antifade Mounting Medium (Vectorlabs H-1000). 30 µl cell suspension was added to a glass section slide and examined by fluorescence microscopy. Non-DAPI stained cells were detected by flow cytometry (BD Accuri™ C6) and analyzed using FlowJo v10.0.8.

Statistics

Statistical analysis was performed using GraphPad Prism version 6.02. P values were determined using Welch-corrected unpaired t-tests or one-way Anova Tukey's multiple comparisons test. Ns: no significance. *P<0.05, **P<0.01, ***P<0.001, ****P<0.0001.

Results

HPV-infected KCs have an altered expression of genes related to necroptosis and proliferation in response to IFNγ and TNFα stimulation.

We previously reported our validated microarray in which four independent uninfected KC and four independent hrHPV-infected KC cultures were stimulated with control or IFNγ [14, 31]. Analysis of marker genes in this array for necroptosis (*RIPK3, MLKL*), proliferation (*RARRES1, PCNA*), intrinsic apoptosis (*BCL-2, BAX*), extrinsic apoptosis (*FADD, CFLAR*) and senescence (*GLB1, DEP1*) revealed that hrHPV-infection was specifically associated with changes in the genes associated with necroptosis and proliferation (Figure 1A). *RIPK3*, a crucial regulator of necroptosis, and its downstream partner *MLKL* [35] were both down-regulated in IFNγ-stimulated hrHPV-infected KCs (Figure 1A). Furthermore, the increase in *RARRES1*, a marker for anti-proliferation [36, 37], and the decrease in *PCNA*, a marker of proliferation, observed in KCs treated with IFNγ for 24 hours was not seen in hrHPV-positive KCs where expression of these genes remained almost unaltered (Figure 1A). These data suggest that hrHPV-infected KCs can resist the growth regulatory effects of IFNγ and/or the combination of IFNγ and TNFα. Uninfected KCs and hrHPV-infected KCs express the IFNγ receptor 1 (IFNGR1), and the TNFα receptors 1 and 2 (TNFR1 and TNFR2) at the cell surface enabling them to respond to these cytokines (Supplemental Figure 1A). When these cells were seeded into 96-well plates and treated for four days with increasing doses of IFNγ and/or TNFα, the growth of uninfected KCs was greatly affected by IFNγ in a dose-dependent manner while hrHPV-positive KCs were much more resistant to growth inhibition and still able to expand to a confluent cell layer (Supplemental Figure 1B). TNFα in itself appeared not to affect the growth of uninfected or HPV-infected KCs, but when combined with IFNγ it exaggerated the reduction in cell density (Supplemental Figure 1B). To confirm these results, KCs were harvested after IFNγ/TNFα stimulation, and the gene expression of the previously indicated markers indicative for proliferation, senescence, apoptosis and necroptosis were determined by RT-qPCR (Figure 1B). The qPCR showed that *RIPK3* is lower in hrHPV-infected KCs both at the basal level and after

treatment, while the effect on *MLKL* was less pronounced. Moreover, the increase in *RARRES1* and downregulation of *PCNA* was much lower in treated hrHPV-infected KC than in non-infected KCs (**Figure 1B**). Similar to the microarray, the marker genes for intrinsic and extrinsic apoptosis as well as senescence did not overtly differ between KCs and hrHPV-positive KCs. Together, our results show that specifically the necroptosis associated gene *RIPK3* and the anti-proliferative gene *RARRES1* were expressed lower in hrHPV-positive KCs. This suggests that the maintained proliferation of hrHPV-infected undifferentiated KCs during IFNγ and/or TNFα treatments is associated with a resistance to cell death at the level of necroptosis and by resistance to proliferation arrest but less likely to be regulated at the level of senescence or apoptosis.

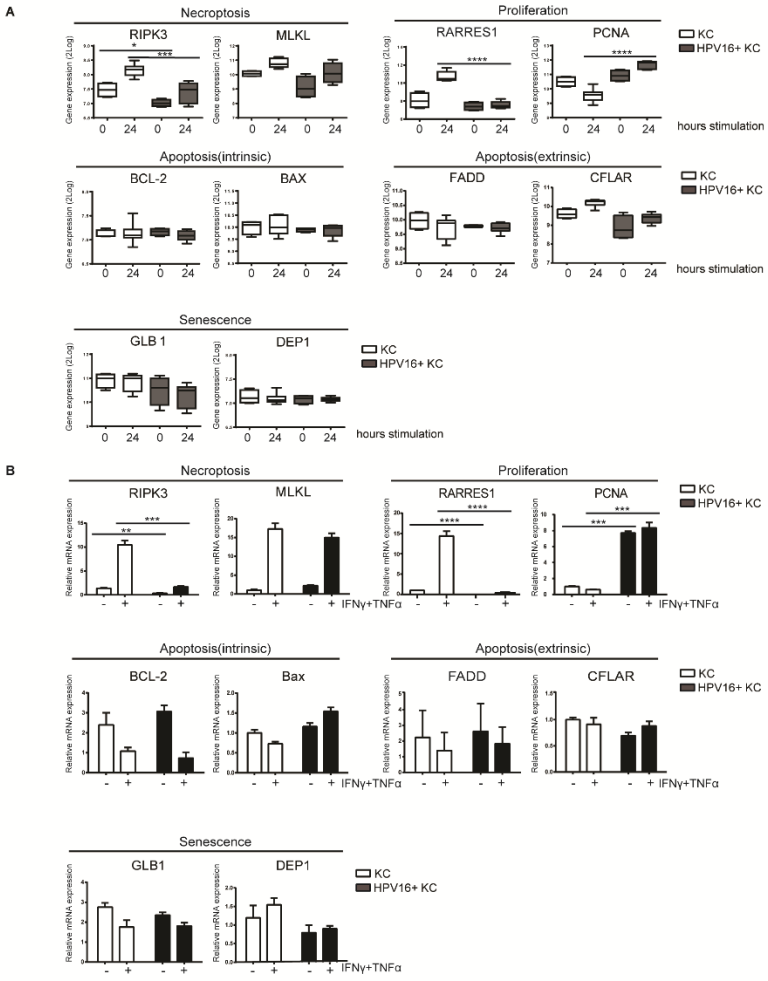

Figure 1. HPV-infected KCs display an altered expression of genes related to necroptosis and proliferation.

(A) Microarray gene expression values for *RIPK3, MLKL, RARRES1, PCNA, BCL-2, BAX, FADD, CFLAR, GLB1* and *DEP1* of 4 independent uninfected KCs and 4 independent hrHPV+ KCs, stimulated with IFNγ for 0 or 24 hours, represented in a box plot. The box represents the 25th and 75th percentiles, the median is indicated with a horizontal line within the box, and the whiskers represent the minimum and maximum. ***P<0.001 and ****P<0.0001.

(B) RT-qPCR *of RIPK3, MLKL, RARRES1, PCNA, BCL-2, BAX, FADD, CFLAR, GLB1* and *DEP1* in uninfected KCs and HPV16+KCs following treatment with 50 IU/ml IFNγ and 30 ng/ml TNFα for 24 hours. Gene expression was normalized against *GAPDH* mRNA levels and standardized against the non-stimulated uninfected KCs. Similar results were observed in two independent experiments. ****P<0.0001.

HPV suppresses necroptosis by downregulating RIPK3 expression.

Programmed cell death knows two major regulatory pathways: caspase-dependent apoptosis and RIP kinases-associated necroptosis [38]. To investigate the effects of hrHPV on these pathways, we analyzed the expression of the proteins TRAF2, cIAP1, cIAP2, XIAP, FLIP, CYLD, caspase-8, FADD, RIPK1, RIPK3, and MLKL, involved in formation of the apoptotic or necroptotic signaling complexes [38] at several different time points after IFNγ/TNFα stimulation (Figure 2). We found a consistent difference between KCs and hrHPV-positive KCs with respect to cIAP2, the expression of which was strongly upregulated at both the protein and transcript level by IFNγ/TNFα stimulation in hrHPV-positive KCs only (Figures 2A and 2D). The cytokine-stimulated expression of TRAF2 seemed to be higher in hrHPV-positive KCs but this was not confirmed at the transcript level (Figures 2A and 2D). Analysis of the apoptotic (FLIP, CYLD, caspase-8, FADD) or necroptotic (RIPK1, RIPK3, MLKL) proteins revealed that the levels of FADD were consistently upregulated in hrHPV-positive KCs in response to IFNγ/TNFα treatment. Again, this was not confirmed at the transcript level (Figures 2B and 2D). Similarly, there was a hint that cFLIP was upregulated at the protein level but not at the transcript level (Figures 2B and 2D). In addition, there was no difference between the different KCs in the expression caspase-8 or in the expression of partially cleaved caspase-8 (43 kD) after IFNγ/TNFα treatment (Figure 2B). Fully cleaved caspase-8 (18 kD and 10 kD) was not observed in these blots, unless KCs and hrHPV+KCs were treated with cyclohexamide, which fosters apoptosis by promoting full caspase-8 activation via the elimination of c-FLIP [39] (Supplemental Figure 2). Importantly, RIPK3 was downregulated significantly at the

protein level and transcript level by hrHPV (Figures 2C and 2D). Note that in hrHPV-positive KCs the increase in phosphorylated MLKL parallels that of MLKL itself and does not reflect a specific increase in MLKL phosphorylation (Figure 2C). Notably, the expression of many of the proteins in the apoptotic and necroptotic signaling complexes could be increased by either IFNγ or TNFα but most often the two cytokines synergized in raising the expression of these proteins, in particular RIPK3 (Supplemental Figure 3). The expression of the other components showed a similar expression in non-infected or hrHPV-positive KCs or varied between cell lines in a non-HPV related manner. To study the role of HPV in the consistently changed components cIAP2, FADD and RIPK3, the total HPV16 early gene expression was knocked down by introduction of siRNA against HPV16 E2 in hrHPV+KCs [13]. This resulted in the reduction of HPV16 gene expression in non- and IFNγ TNFα stimulated hrHPV+ KC (Figure 2E) as well as in the upregulation of *RIPK3* and unexpectedly also of *cIAP2,* while there was no change in *FADD* (Figure 2F). IFNγ TNFα stimulation augmented the expression of *cIAP2* and *RIPK3* in KCs when the polycistronic mRNA of HPV16 was knocked down (Figure 2F). These data indicate that only the altered expression of *RIPK3,* but not that of *cIAP2* and *FADD*, can be fully accounted for by an infection of KCs with hrHPV and suggest that hrHPV might impair IFNγ and TNFα induced necroptosis.

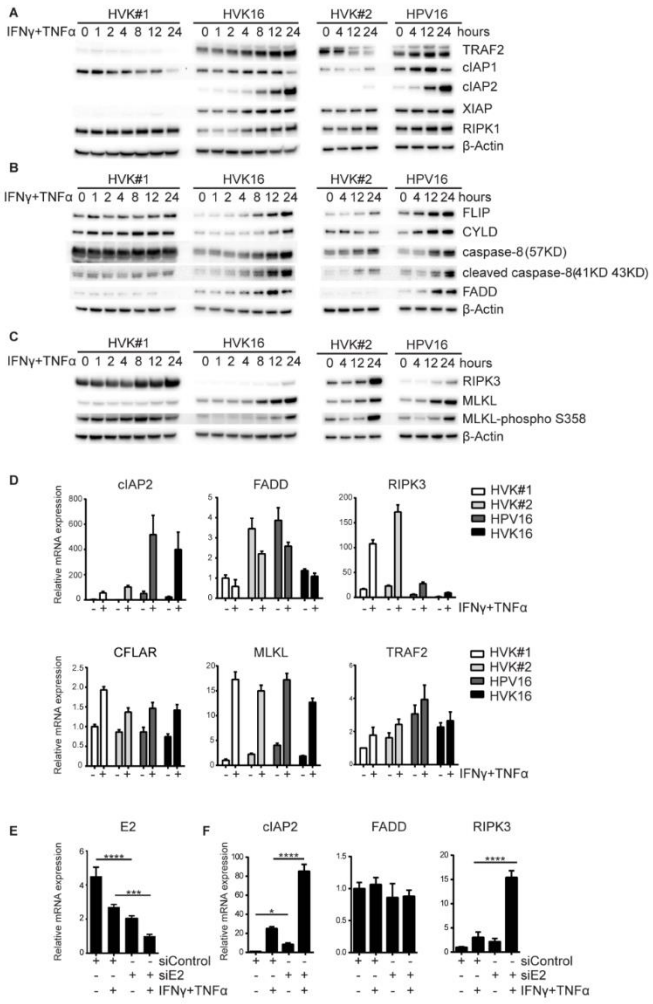

Figure 2. HPV suppresses the expression of RIPK3.

(A-C) Two independent uninfected KC cultures (HVK#1, HVK#2) and two HPV16+KC cultures (HVK16, HPV16) were stimulated with 50 IU/ml IFNγ and 30 ng/ml TNFα for the indicated times. The protein expression levels of (A) TRAF2, cIAP1, cIAP2, XIAP, RIP1 and (B) FLIP, CYLD, caspase-8 (57 kD), cleaved caspase-8 (41 kD, 43 kD), FADD, and (C) RIPK3, MLKL and MLKL-phospho S358 as detected by western blotting (WB) in whole cell extracts. β-actin served as loading control.

(D) Two independent uninfected KC cultures (HVK#1, HVK#2) and two HPV16+KC cultures (HVK16, HPV16) were stimulated with 50 IU/ml IFNγ and 30 ng/ml TNFα for 24 hours after which the expression levels of *cIAP2, FADD, RIPK3, CFLAR, MLKL* and *TRAF2* were determined by RT-qPCR. Gene expression was normalized against *GAPDH* mRNA levels and standardized against the non-stimulated HVK#1. Similar results were observed in two independent experiments.
(E) HPV16 *E2* expression in HPV+KCs transfected with control siRNA (siControl) or siRNA targeting HPV16 E2 (siE2) stimulated with or without 50 IU/ml IFNγ and 30 ng/ml TNFα for 24 hours. *E2* expression was analyzed by RT-qPCR. Gene expression was normalized against *GAPDH* mRNA levels and standardized against siControl. Similar results were observed in 3 independent experiments. ***P<0.001 and ****P<0.0001.
(F) Expression of *cIAP2, FADD* and *RIPK3* in hrHPV+ KCs transfected with control siRNA (siControl) or siRNA targeting HPV16 E2 (siE2) stimulated with or without 50 IU/ml IFNγ and 30 ng/ml TNFα for 24 hours. Gene expression was normalized against *GAPDH* mRNA levels and standardized against siControl. Similar results were observed in 2 independent experiments. *P<0.05, ****P<0.0001

To test this, KCs and hrHPV-positive KCs were stimulated for 48 hours with IFNγ and TNFα in the presence of the Smac mimetic BV6 and caspase inhibitor zVAD-fmk in order to promote necroptosis [40] and cell death was analyzed with SYTOX green dead cell stain. While about 80% of the non-infected KCs were killed, a significantly lower percentage, less than 40%, of the hrHPV+KCs died within this 48 hour time frame (Figure 3). Consistent with necroptosis, cell death was completely blocked when the RIP kinase 1 inhibitor necrostatin (Nec)-1s [41] was present during stimulation (Supplemental Figure 4). Together, these results show that hrHPV-infected KCs can escape from IFNγ/TNFα induced necroptosis by downregulating the basal and cytokine-induced expression of RIPK3.

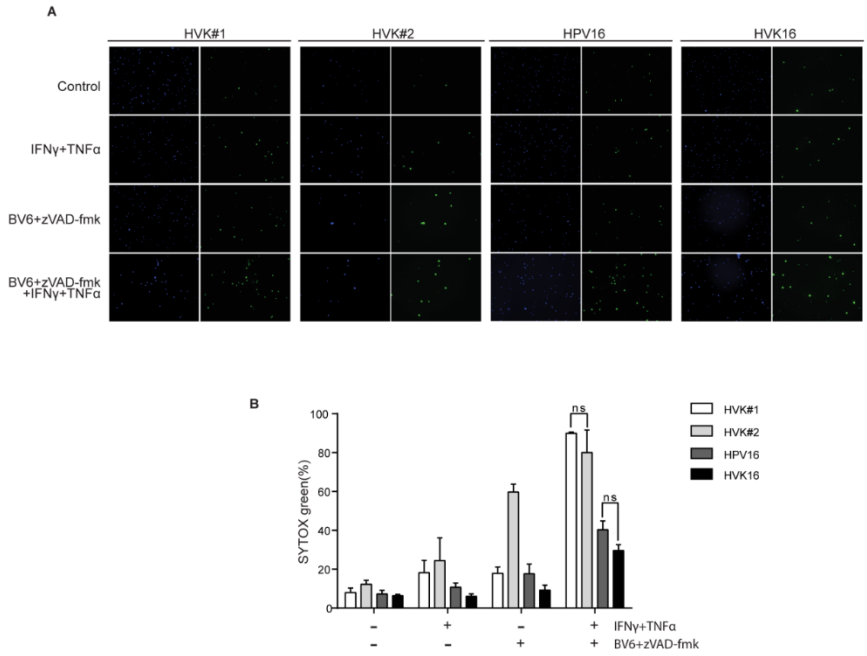

Figure 3. HPV increases the resistance of KCs to necroptosis.
(A) The two independent uninfected KC cultures (HVK#1, HVK#2) and two HPV16+ KC cultures (HVK16,HPV16) were stimulated with 250 IU/ml IFNγ, 250 ng/ml TNFα, 5 µM BV6, and 20 µM zVAD-fmk as indicated for 48 hours. All cell nuclei were labelled with DAPI (blue fluorescence). Dead cells were stained using SYTOX green dead cell stain resulting in green fluorescent nuclei of dead cells.
(B) The number of dead cells among all cells were counted in multiple fields. The percentage of cell death was calculated. P values were determined using one way anova Tukey's multiple comparisons test. In the group of IFNγ+TNFα+BV6+z-VAD-fmk, HVK#1 vs. HPV16, $P<0.01$; HVK#1 vs. HVK16, $P<0.001$; HVK#2 vs. HPV16, $P<0.05$; HVK#2 vs. HVK16, $P<0.05$

RIPK3 downregulation and resistance to necroptosis involves histone methyltransferases overexpressed in hrHPV-infected KCs

In many cancer cell lines the expression of RIPK3 is lost due to genomic methylation near its transcriptional start site [42]. Recently, it was reported that the methyltransferase EZH2 was overexpressed in HPV16 E6 and E7-transformed KCs [43]. Since EZH2 is a core component of polycomb repressive complex 2 (PRC2) and plays a role in promoter-targeted transcriptional repression [44], we hypothesized that EZH2 may also be involved in repressing the expression of *RIPK3*. Western blot analysis and RT-qPCR of primary KCs and hrHPV-infected KCs revealed that both gene and protein expression of EZH2 was higher at the basal level and after IFNγ/TNFα stimulation in hrHPV+KCs (Figures 4A and 4B). As expected [44], hrHPV-infected KCs display a higher methylation of H3K27 at the basal level (Supplemental Figure 5A). Knock-down of the polycistronic mRNA of HPV16 in hrHPV16-positive KCs resulted in lower EZH2 protein levels indicating that EZH2 overexpression was induced by hrHPV in KCs Figure 4C). This effect was even more pronounced after IFNγ/TNFα stimulation fitting with the observation that also the expression of the viral genes was further downregulated (Figure 2E). The use of 3-deazaneplanocin A (DZNep), an inhibitor of S-adenosylmethionine-dependent methyltransferase, is known to effectively deplete cellular levels of the PRC2 components, including EZH2 [45]. Indeed, treatment of the hrHPV+KCs with DZNep resulted in a dose-dependent decrease in EZH2 protein levels (Figure 4D), decreased of H3K27 methylation (Supplemental Figure 5B) and the concomitant increase in RIPK3 at the protein and gene expression level (Figures 4D and 4E). Treatment of hrHPV+KCs with the catalytic EZH2 inhibitor GSK503 did not have a clear effect on the expression of RIPK3 (Supplemental Figure 5C), suggesting that the hrHPV-induced overexpression of EZH2 is indirectly responsible for suppressing RIPK3 mediated necroptosis it should be noted that DZNep has been reported to function as a global histone methylation inhibitor [46]. We therefore analyzed the expression of other methyltransferases and found that, in addition to EZH2, 8 other methyltransferases were expressed at a significantly higher level in hrHPV+KCs (Supplemental Figure 5DE). Potentially, these methyltransferase may also play a role in downregulating the expression of RIPK3. To test if

methyltransferases where involved in suppressing RIPK3-mediated necroptosis, KCs and hrHPV+KCs again were stimulated with IFNγ/TNFα, BV6 and zVAD-fmk but now either in the absence or presence of DZNep. Cell death was determined both by flow cytometry in order to analyze larger numbers of cells (Figure 4F), and by immunofluorescence in cell cultures (Supplemental Figure 6). Clearly, the presence of DZNep increased the BV6/zVAD-fmk/IFNγ/TNFα-induced percentage of dead cells. Cells died by necroptosis, since cell death could be blocked by necrostatin (Nec)-1s (Figures 4F and 4G; Supplemental Figure 6).

Thus, by upregulating the expression of histone methyltransferases, thereby effectively decreasing the basal levels of RIPK3, hrHPV increases the immune resistance of KCs to IFNγ/TNFα stimulated necroptotic cell death.

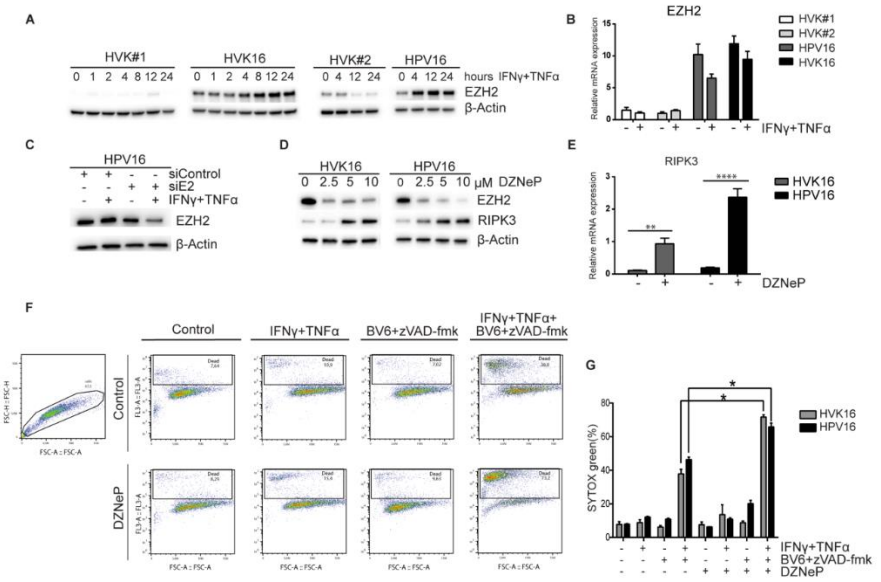

Figure 4. High risk HPV-infected KCs overexpress EZH2 and downregulates RIPK3 and to resist necroptosis.

(A) Two independent uninfected KC cultures (HVK#1, HVK#2) and two HPV16+KC cultures (HVK16, HPV16) were stimulated with 50 IU/ml IFNγ and 30 ng/ml TNFα for the indicated times following the protein

levels of EZH2 as detected by western blotting (WB) in whole cell extracts. β-actin served as loading control.
(B) Two independent uninfected KC cultures (HVK#1, HVK#2) and two HPV16+KC cultures (HVK16, HPV16) were stimulated with 50 IU/ml IFNγ and 30 ng/ml TNFα for 24 hours after which the expression levels of *EZH2* was determined by RT-qPCR. Gene expression was normalized against *GAPDH* mRNA levels and standardized against the non-stimulated uninfected KC culture HVK#1.
(C) The protein expression level of EZH2 was analyzed in HPV16+KCs (HPV16) transfected with control siRNA (siControl) or siRNA targeting HPV16 E2 (siE2) and stimulated with or without 50 IU/ml IFNγ and 30 ng/ml TNFα for 24 hours, using western blotting (WB) in whole cell extracts. β-actin served as loading control.
(D) The protein expression levels of EZH2 and RIPK3 were analyzed in the two independent hrHPV+KCs (HVK16, HPV16) either 72 hours after pharmacological depletion of EZH2 by increasing doses of 3-deazaneplanocin (DZNeP) .
(E) The gene expression level of *RIPK3* in 10μM DZNeP-treated HVK16 and HPV16 hrHPV+ KCs after 72 hours. Gene expression was normalized against *GAPDH* mRNA levels and standardized against the non-treated HVK16. **P<0.01, ****P<0.0001.
(F,G) Two hrHPV+ KCs (HVK16, HPV16) were treated with or without 10 μM DZNeP. After 24 hours, the cells were treated with 250 IU/ml IFNγ, 250 ng/ml TNFα, 5 μM BV6, 20 μM zVAD-fmk and/or 20 μM Nec-1s as indicated for 48 hours. The percentage of dead cells, indicated by the cells stained positive by SYTOX green dead cell stain, was measured by flow cytometry. (F) Example of analysis by flow cytometry. (G) The percentage of cell death measured for each treatment was plotted for both hrHPV+ KC cultures. **P < 0.05.

The anti-proliferative effects of IFNγ in KCs are counteracted by hrHPV through downregulation of interferon-induced transmembrane protein 1 (IFITM1).

Our initial analyses suggested that hrHPV-infected KCs resisted immune-controlled cell growth not only via impairment of necroptosis but also by interfering with regulation of proliferation,

exemplified by a lower increase in *RARRES1* and downregulation of *PCNA* (Figure 1). Indeed, stimulation of non-infected KCs and hrHPV+KCs with a high dose of IFNγ affects the growth of non-infected KCs but not hrHPV+KCs (Figure 5A). Furthermore, analysis of the cell cycle using flow cytometry and propidium iodide DNA staining, showed that treatment of KCs with IFNγ caused a 50% reduction in the S-phase while it hardly affected hrHPV+KCs (Figures 5B and 5C).

IFNγ signaling requires STAT1 and it has been reported that HPV can lower *STAT1* expression and protein levels in KCs [4-7], potentially explaining the resistance to IFNγ treatment. Indeed, hrHPV-positive KCs displayed a lower expression of STAT1 at the protein level (Figure 5D; Supplemental Figure 7), and this was due to the presence of hrHPV as knock-down of the polycistronic viral mRNA resulted in a higher *STAT1* expression (Figure 5E). Notably, cytokine stimulation also upregulated *STAT1* expression (Figure 5E), and IFNγ stimulation resulted in high levels of phosphorylated STAT1 in hrHPV+KCs (Figure 5D), indicating that HPV may repress the basal levels of STAT1 but it does not overtly interfere with STAT1 signaling *per se*. This also explains why IFNγ, especially at higher concentrations and in combination with TNFα, is able to stimulate the expression of the anti-proliferative gene *RARRES1* and downregulation of the proliferative gene *PCNA* (Figure 5F), albeit that the combinatory effects of IFNγ and TNFα were more pronounced on non-infected KCs (Figure 5F).

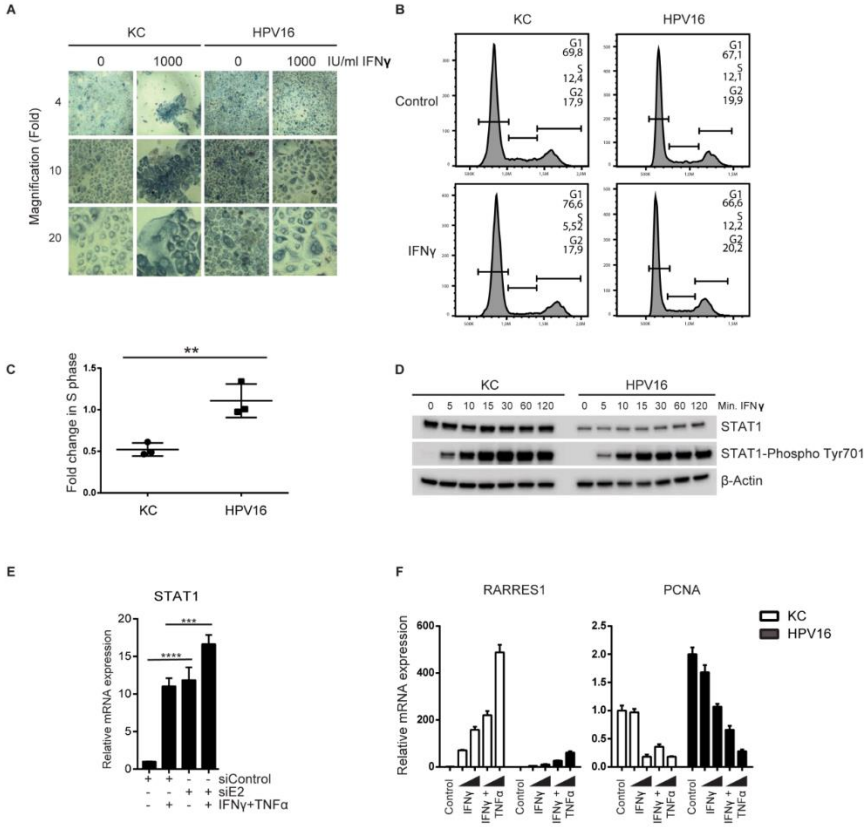

Figure 5. High-risk HPV resists the anti-proliferative effects of IFNγ.

(A) Undifferentiated KCs (HVK#1) and HPV16+KCs (HVK16) were treated with indicated doses of IFNγ for 72 hours after which cell confluency was monitored by phase-contrast microscopy as a measure of proliferation. Microscopy pictures (4x, 10x and 20x magnifications).

(B,C) The proliferation of undifferentiated KC (HVK#2) and HPV16+KC (HPV16) treated with 250 IU/ml IFNγ for 48 hours was analyzed by examination of the proportion of DNA that was present in the various

phases (G1, S, G2/M) of cell growth using PI staining and flow cytometry. (B) Example of flow cytometric analysis. The DNA content of 10,000 cells was analyzed. (C) The fold change in the percentage of cells in the S phase of treated cells over non-treated cells of n=3 experiments is shown. **P<0.01.
(D) The protein levels of STAT1 and phosphorylated STAT1 at Tyr701 protein levels in undifferentiated KCs and HPV16+KCs harvested at indicated time points after stimulation with 50 IU/ml IFNγ as measured by WB is shown. β-actin served as loading control.
(E) Expression of *STAT1* in HPV16+ KCs transfected with control siRNA (siControl) or siRNA targeting HPV16 E2 (siE2) stimulated with or without 50 IU/ml IFNγ and 30 ng/ml TNFα for 24 hours. Gene expression was normalized against *GAPDH* mRNA levels and fold-change over non-stimulated siControl was calculated. ****P<0.0001, ***P<0.001.
(F) Gene expression analysis of *RARRES1* and *PCNA* in undifferentiated KCs and HPV16+ KCs treated with 50 IU/ml IFNγ and 30 ng/ml TNFα for 24 hours. Gene expression was normalized against *GAPDH* mRNA levels and fold change over control was calculated.

IFITM1 plays an essential role in the anti-proliferative action of IFNγ [47], making it a potential target for hrHPV. Re-analysis of the data from one of our earlier validated microarrays, in which the basal expression of genes measured in different uninfected and hrHPV infected KCs was compared in the absence of IFNγ stimulation [31], showed that *IFITM1* expression is downregulated in HPV-positive KCs (Figure 6A). This was confirmed by RT-qPCR (Figure 6B). To show that the expression of IFITM1 was genuinely altered by the presence of hrHPV in KCs, undifferentiated KCs were infected with native HPV16 virions resulting in a reduced expression of *IFITM1* (Figure 6C). Reciprocally, the knock-down of total HPV16 early gene expression in hrHPV+KCs resulted in the upregulation of *IFITM1* (Figure 6D). IFNγ induces *de novo* synthesis of *IFITM1* for which STAT1 is required [48-51]. Indeed, IFNγ stimulation of uninfected KCs resulted in approximately 4-fold increase in *IFITM1* after 24 hours (Figure 6E). Strikingly, IFNγ stimulation of hrHPV+KCs resulted in a much stronger

relative increase of IFITM1 levels (Figure 6F), albeit that these levels still remained lower than those measured in uninfected KCs (Figure 6E). IFITM1 protein levels in IFNγ-stimulated KCs and hrHPV+KCs confirmed the gene expression data (Figure 6G). These data indicated that hrHPV predominantly regulates the expression of *IFITM1* at the basal level but less at the level of IFNγ-mediated induction of *IFITM1* gene expression. Interestingly, the hrHPV+KCs with the highest basal IFITM1 protein expression also showed the highest STAT1 levels (Supplemental Figure 7). TNFα did not influence *IFITM1* expression (Figures 6E and 6F).

To study the effects of IFITM1 on KC proliferation in a setting where all additional influences of HPV are ruled out [52, 53], IFITM1 was knocked-down in uninfected KCs (Figure 6H). The KCs were stimulated with IFNγ or IFNγ/TNFα. The basal level of *RARRES1* was lower in IFITM1 knocked-down KCs and its IFNγ-induced expression was clearly affected when KCs were stimulated with a low concentration of IFNγ (Figure 6I). A higher concentration of IFNγ overcame the effect of IFITM1 knock-down on the expression of *RARRES1*. In addition, IFITM1 knock-down KCs displayed a less strong downregulation of *PCNA* upon IFNγ stimulation (Figure 6I). The less pronounced effects on *RARRES1* and *PCNA* at the higher IFNγ concentrations used was probably due to the fact that upon IFNγ stimulation still an increase in *IFITM1* could be observed in IFITM1 knock-down KCs (Figure 6I). In addition, control shRNA-transduced KCs were less resistant than IFITM1 knock-down KCs to the anti-proliferative effects of IFNγ and the combination of IFNγ and TNFα when cell confluency was monitored by phase-contrast microscopy or cell number was quantitated by a DNA-based proliferation assay (Supplemental Figure 8AB). Thus, HPV is able to resist IFNγ-mediated arrest of proliferation by lowering the basal levels of IFITM1.

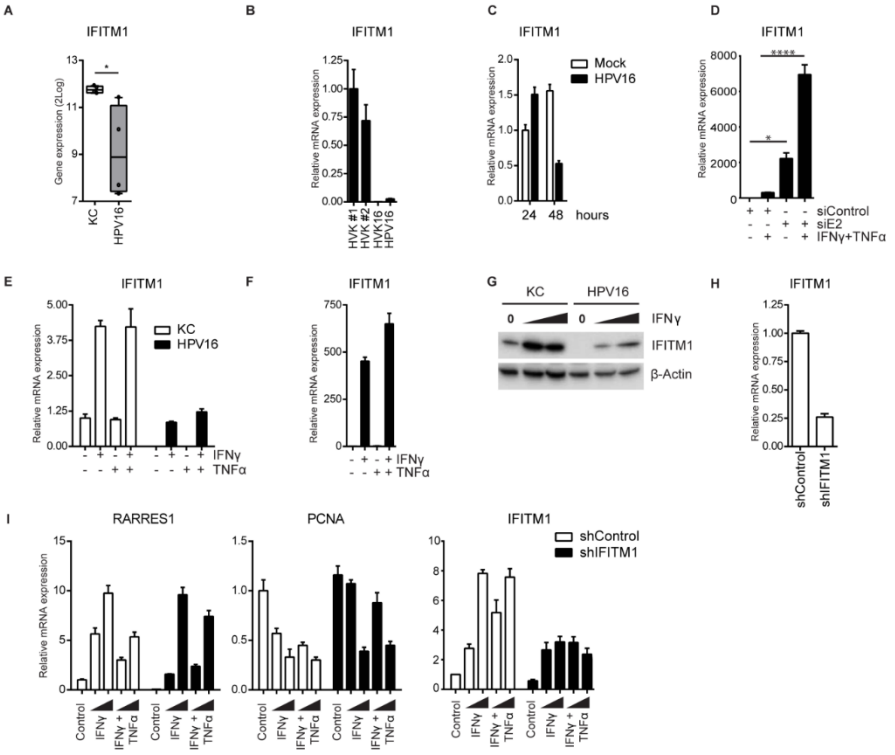

Figure 6. High-risk HPV-infected KCs downregulate IFITM1 to suppress the expression of *RARRES1* and to maintain proliferation.

(A) Microarray gene expression values for *IFITM1* in 4 independent uninfected KCs and 4 independent hrHPV+KCs represented in a box plot. * p<0.05.

(B) The expression level of *IFITM1* in HVK#1, HVK#2, HVK16 and HPV16 determined by RT-qPCR. Gene expression was normalized against *GAPDH* mRNA levels.

(C) The expression level of *IFITM1* in KCs infected with mock or native HPV16 virions for 1 or 2 days, respectively.

(D) Expression of *IFITM1* in HPV16+KCs transfected with control siRNA (siControl) or siRNA targeting HPV16 E2 (siE2) stimulated with or without 50 IU/ml IFNγ and 50 ng/ml TNFα for 24 hours. Gene expression was normalized against *GAPDH* mRNA levels and fold-change over non-stimulated siControl was calculated. *P<0.05, ****P<0.0001.

(E, F) The expression of *IFITM1* in undifferentiated KCs and HPV16+KCs stimulated with 50 IU/ml IFNγ and/or 50 ng/ml TNFα for 24 hours. Gene expression was normalized against *GAPDH* mRNA levels and fold changes over (E) control-stimulated undifferentiated KCs or over (F) control-stimulated HPV16+KCs were calculated and depicted.
(G) IFITM1 protein levels in KC and HPV16+KC stimulated with 0, 100 or 1000 IU/ml IFNγ, as measured by WB. β-actin served as loading control.
(H) *IFITM1* expression in control and IFITM1 knockdown uninfected KCs as measured by RT-qPCR. Gene expression was normalized against *GAPDH* mRNA levels and fold-change over siControl was calculated.
(I) Control and *IFITM1* knockdown KCs were stimulated with 50 IU/ml IFNγ and/or 50 ng/ml TNFα for 24 hours before the expression of *RARRES, PCNA, and IFITM1* was measured by RT-qPCR. Gene expression was normalized against *GAPDH* mRNA levels and fold-change over non-stimulated shControl was calculated.

Discussion

In most cases the immune system succeeds in controlling hrHPV infections but this process takes time and requires the presence of strong IFNγ and TNFα-associated HPV-specific T cell responses [16]. Here we show that hrHPV-infected KCs resist the immune system by interfering with the regulation of intracellular growth and cell death programs of infected cells. Under normal circumstances these would be activated in response to the effector molecules of the adaptive immune system and function as a host defense mechanism to control viral spread [54]. Using a unique *in vitro* model we showed that hrHPV infection renders KCs resistant to IFNγ/TNFα-induced necroptosis and arrest of cell growth. HrHPV infection is associated with the upregulation of 9 methyltransferases, including EZH2, and downregulation of the expression of RIPK3 which results in an impaired induction of necroptosis by IFNγ/TNFα stimulation. Use of DZNep, a global inhibitor of methyltransferases and a pharmacological compound that depletes EZH2 [45, 46], restored the expression of RIPK3 and the sensitivity of hrHPV-infected KCs to IFNγ/TNFα-mediated necroptosis. Use of the catalytic EZH2 inhibitor GSK503 did restore RIPK3 expression, suggesting that either EZH2 is indirectly responsible for suppressing RIPK3 mediated necroptosis or that one or more of the other overexpressed methyltransferases are involved in the downregulation of RIPK3. Furthermore, hrHPV effectively downregulated the basal expression of the negative regulator of cell growth *IFITM1,* resulting in an impaired IFNγ-mediated increase in the expression of the anti-proliferative *RARRES1* gene and decrease of the proliferative gene *PCNA* as well as impaired arrest of cells in the S-phase. Knockdown of *IFITM1* with siRNA in normal KCs recapitulated the effects on *RARRES1* and *PCNA* expression and cell proliferation observed in hrHPV+KCs.

Apoptosis and necroptosis play an important role in controlling viral infections [54]. We did not observe any HPV-induced differences in the expression of caspase-8, FLIP or FADD, nor did we observe differences in cleavage of caspase-8 upon stimulation with IFNγ and TNFα. Notably, stimulation with IFNγ and TNFα did not lead to

activation of caspase-8, reflected by the absence of fully cleaved caspase-8 in undifferentiated normal or hrHPV-positive KCs. However, upon differentiation KCs become sensitive to Fas- and caspase-8-mediated apoptosis following stimulation with IFNγ and TNFα [29, 30]. In contrast, stimulation of undifferentiated KCs did result in necroptosis following an increase of RIPK3, most notably when both IFNγ and TNFα were used. The induction of necroptosis has shown to be important for the control of vaccinia virus [55] and herpes simplex virus type 1 [56]. Consequently, viruses have developed strategies to resist this immune control mechanism. The murine cytomegalovirus expresses the M45-encoded inhibitor of RIP activation (vIRA), that targets RIPK3 and disrupts RIPK1-RIPK3 interactions characteristic for necroptosis [57]. Rather than by interrupting necroptosis, hrHPV prevents the formation of the necrosome by reducing the levels of RIPK3 via the upregulation of histone methyltransferases.

The production of new HPV particles requires proliferation and differentiation of infected basal KCs. An arrest in cell proliferation, therefore, is an effective means to control viral infection. IFITM1 plays an essential role in the anti-proliferative action of IFNγ [47], thus lowering its expression – as observed in hrHPV-infected KCs – may allow viral escape. Indeed, hepatitis C virus was found to decrease the expression of *IFITM1* via the upregulation of mIR-130a in order to sustain its replication [58]. We showed that the basal expression of *IFITM1* is downregulated in hrHPV+KCs, but its downstream partner *RARRES1* is not. This might be explained by the fact that the basal expression of *RARRES1* in uninfected KCs is already low. The IFNγ-induced increase in expression of *IFITM1* and *RARRES1* requires signaling via the IFNGR1 and STAT1. Overexpression of EZH2 has been reported to suppress the expression of IFNGR1 in MYC- but not phosphatidylinositol 3-kinase (PI3K)-transformed cells, despite the fact that in both types of transformed cells EZH2 was overexpressed [59]. Notwithstanding the ectopic expression of EZH2 in hrHPV-positive KCs, there were no specific differences in the expression of IFNGR1 between non-infected and hrHPV-positive cells. This is in line with the observation that the PI3K pathway is a major target for the

hrHPV proteins [59, 60] and suggests that the overexpression of EZH2 does not play a role in the escape of hrHPV-positive cells at this level. It was previously reported that the HPV early proteins E6 and E7 downregulate the expression of STAT1 [4-6]. Our data confirm that infection with hrHPV decreases basal STAT1 protein levels in KCs but also show that hrHPV does not interfere with IFNγ-induced STAT1 activation *per se*, as reflected by STAT1 phosphorylation and increase in *RARRES1* and *IFITM1* expression. Still, as total STAT1 levels are lower in hrHPV+KCs, the reduced total amount of activated STAT1 may explain why in hrHPV+KCs the increase in *RARRES1* and *IFITM1* expression does not reach the levels observed in uninfected KCs. This is also demonstrated by the data showing that the effect of *IFITM1* knock-down on proliferation of uninfected KCs is not similar to what hrHPV has on KCs. Whilst the effect of IFITM1 in uninfected KCs is apparent and anti-proliferative, indicated by the retained expression of *PCNA* and *RARRES1* in KCs stimulated with a low dose of IFNγ when *IFITM1* was knocked-down, clearly the downregulation of STAT1 as well as the positive growth signals as delivered by hrHPV [52, 53] are missing in these cells. Hence, differences in IFNγ-stimulated arrest of proliferation are less noticeable. This shows that, whereas the decreased basal level of *IFITM1* is already providing resistance to the IFNγ-stimulated arrest of proliferation, the downregulation of STAT1 is likely to exaggerate this effect. Mechanistically, IFITM1 inhibits the phosphorylation of ERK and thereby regulates mitogen-activated protein (MAP) kinase signaling. Furthermore, IFITM1 mediates the de-phosphorylation of p53 at Thr55, resulting in increased p53 stability and transcriptional activity, and the upregulated expression of p21. Consequently, there is an arrest in cell cycle progression and hence a stop in proliferation [47]. This was also observed in this study and reflected by the retained *PCNA* expression when *IFITM1* was knocked-down in low dose IFNγ-stimulated KCs.

In conclusion, hrHPV controls proliferation by regulating the expression of (anti-)proliferative genes via STAT1 and IFITM1 and resists the induction of necroptotic cell death by downregulation of RIPK3 expression. This allows infected KCs to partly resist immune

pressure by IFNγ/TNFα and explains how hrHPV can partially evade the effector mechanisms of the immune system, which may ultimately lead to progression of hrHPV-induced lesions.

Conflict of Interest

The authors do not declare any conflict of interest.

Author Contributions

Design of study: JB and SVDB
Performed Experiments: WM, BT, RG
Delivered materials: EvE, CM
Analyzed data: WM, BT, RG, JB
Interpreted data: WM, BT, RG, EvE, CM, CJJM, JB, SvdB
Writing: WM, BT, CM, CJMM,JB, SvdB

Acknowledgments

WM is supported by a grant from the China Scholarship Council (201306240016). BT, JMB and SHvdB were supported by the Netherlands Organization for Health Research (NWO/ZonMw) TOP grant 91209012.

References

1. zur Hausen H. Papillomaviruses and cancer: from basic studies to clinical application. Nature reviews Cancer. 2002;2(5):342-50. doi: 10.1038/nrc798. PubMed PMID: 12044010.
2. Doorbar J. Molecular biology of human papillomavirus infection and cervical cancer. Clinical science. 2006;110(5):525-41. doi: 10.1042/CS20050369. PubMed PMID: 16597322.
3. Tummers B, Burg SH. High-risk human papillomavirus targets crossroads in immune signaling. Viruses. 2015;7(5):2485-506. doi: 10.3390/v7052485. PubMed PMID: 26008697; PubMed Central PMCID: PMC4452916.
4. Chang YE, Laimins LA. Microarray analysis identifies interferon-inducible genes and Stat-1 as major transcriptional targets of human papillomavirus type 31. Journal of virology. 2000;74(9):4174-82. PubMed PMID: 10756030; PubMed Central PMCID: PMC111932.
5. Hong S, Mehta KP, Laimins LA. Suppression of STAT-1 expression by human papillomaviruses is necessary for differentiation-dependent genome amplification and plasmid maintenance. Journal of virology. 2011;85(18):9486-94. doi: 10.1128/JVI.05007-11. PubMed PMID: 21734056; PubMed Central PMCID: PMC3165741.
6. Nees M, Geoghegan JM, Hyman T, Frank S, Miller L, Woodworth CD. Papillomavirus type 16 oncogenes downregulate expression of interferon-responsive genes and upregulate proliferation-associated and NF-kappaB-responsive genes in cervical keratinocytes. Journal of virology. 2001;75(9):4283-96. doi: 10.1128/JVI.75.9.4283-4296.2001. PubMed PMID: 11287578; PubMed Central PMCID: PMC114174.
7. Zhou F, Chen J, Zhao KN. Human papillomavirus 16-encoded E7 protein inhibits IFN-gamma-mediated MHC class I antigen presentation and CTL-induced lysis by blocking IRF-1 expression in mouse keratinocytes. The Journal of general virology. 2013;94(Pt 11):2504-14. doi: 10.1099/vir.0.054486-0. PubMed PMID: 23956301.
8. Avvakumov N, Torchia J, Mymryk JS. Interaction of the HPV E7 proteins with the pCAF acetyltransferase. Oncogene. 2003;22(25):3833-41. doi: 10.1038/sj.onc.1206562. PubMed PMID: 12813456.
9. Bernat A, Avvakumov N, Mymryk JS, Banks L. Interaction between the HPV E7 oncoprotein and the transcriptional coactivator p300. Oncogene. 2003;22(39):7871-81. doi: 10.1038/sj.onc.1206896. PubMed PMID: 12970734.
10. Caberg JH, Hubert P, Herman L, Herfs M, Roncarati P, Boniver J, et al. Increased migration of Langerhans cells in response to HPV16 E6 and E7 oncogene silencing: role of CCL20. Cancer immunology, immunotherapy : CII. 2009;58(1):39-47. doi: 10.1007/s00262-008-0522-5. PubMed PMID: 18438663.
11. Havard L, Rahmouni S, Boniver J, Delvenne P. High levels of p105 (NFKB1) and p100 (NFKB2) proteins in HPV16-transformed keratinocytes: role of E6 and E7

oncoproteins. Virology. 2005;331(2):357-66. doi: 10.1016/j.virol.2004.10.030. PubMed PMID: 15629778.
12. Huang SM, McCance DJ. Down regulation of the interleukin-8 promoter by human papillomavirus type 16 E6 and E7 through effects on CREB binding protein/p300 and P/CAF. Journal of virology. 2002;76(17):8710-21. PubMed PMID: 12163591; PubMed Central PMCID: PMC136974.
13. Karim R, Tummers B, Meyers C, Biryukov JL, Alam S, Backendorf C, et al. Human papillomavirus (HPV) upregulates the cellular deubiquitinase UCHL1 to suppress the keratinocyte's innate immune response. PLoS pathogens. 2013;9(5):e1003384. doi: 10.1371/journal.ppat.1003384. PubMed PMID: 23717208; PubMed Central PMCID: PMC3662672.
14. Tummers B, Goedemans R, Jha V, Meyers C, Melief CJ, van der Burg SH, et al. CD40-Mediated Amplification of Local Immunity by Epithelial Cells Is Impaired by HPV. The Journal of investigative dermatology. 2014. doi: 10.1038/jid.2014.262. PubMed PMID: 24945092.
15. Tummers B, Goedemans R, Pelascini LP, Jordanova ES, van Esch EM, Meyers C, et al. The interferon-related developmental regulator 1 is used by human papillomavirus to suppress NFkappaB activation. Nature communications. 2015;6:6537. doi: 10.1038/ncomms7537. PubMed PMID: 26055519; PubMed Central PMCID: PMC4382698.
16. van der Burg SH, Melief CJ. Therapeutic vaccination against human papilloma virus induced malignancies. Current opinion in immunology. 2011;23(2):252-7. doi: 10.1016/j.coi.2010.12.010. PubMed PMID: 21237632.
17. Kenter GG, Welters MJ, Valentijn AR, Lowik MJ, Berends-van der Meer DM, Vloon AP, et al. Vaccination against HPV-16 oncoproteins for vulvar intraepithelial neoplasia. The New England journal of medicine. 2009;361(19):1838-47. doi: 10.1056/NEJMoa0810097. PubMed PMID: 19890126.
18. van Poelgeest MI, Welters MJ, Vermeij R, Stynenbosch LF, Loof NM, Berends-van der Meer DM, et al. Vaccination against Oncoproteins of HPV16 for Noninvasive Vulvar/Vaginal Lesions: Lesion Clearance Is Related to the Strength of the T-Cell Response. Clinical cancer research : an official journal of the American Association for Cancer Research. 2016;22(10):2342-50. doi: 10.1158/1078-0432.CCR-15-2594. PubMed PMID: 26813357.
19. Trimble CL, Morrow MP, Kraynyak KA, Shen X, Dallas M, Yan J, et al. Safety, efficacy, and immunogenicity of VGX-3100, a therapeutic synthetic DNA vaccine targeting human papillomavirus 16 and 18 E6 and E7 proteins for cervical intraepithelial neoplasia 2/3: a randomised, double-blind, placebo-controlled phase 2b trial. Lancet. 2015;386(10008):2078-88. doi: 10.1016/S0140-6736(15)00239-1. PubMed PMID: 26386540.
20. Welters MJ, Kenter GG, de Vos van Steenwijk PJ, Lowik MJ, Berends-van der Meer DM, Essahsah F, et al. Success or failure of vaccination for HPV16-positive vulvar lesions correlates with kinetics and phenotype of induced T-cell responses. Proceedings of the National Academy of Sciences of the United States of America.

2010;107(26):11895-9. doi: 10.1073/pnas.1006500107. PubMed PMID: 20547850; PubMed Central PMCID: PMC2900675.
21. Platanias LC. Mechanisms of type-I- and type-II-interferon-mediated signalling. Nature reviews Immunology. 2005;5(5):375-86. doi: 10.1038/nri1604. PubMed PMID: 15864272.
22. Balachandran S, Adams GP. Interferon-gamma-induced necrosis: an antitumor biotherapeutic perspective. Journal of interferon & cytokine research : the official journal of the International Society for Interferon and Cytokine Research. 2013;33(4):171-80. doi: 10.1089/jir.2012.0087. PubMed PMID: 23570383; PubMed Central PMCID: PMC3624769.
23. Thapa RJ, Nogusa S, Chen P, Maki JL, Lerro A, Andrake M, et al. Interferon-induced RIP1/RIP3-mediated necrosis requires PKR and is licensed by FADD and caspases. Proceedings of the National Academy of Sciences of the United States of America. 2013;110(33):E3109-18. doi: 10.1073/pnas.1301218110. PubMed PMID: 23898178; PubMed Central PMCID: PMC3746924.
24. Cabal-Hierro L, Lazo PS. Signal transduction by tumor necrosis factor receptors. Cellular signalling. 2012;24(6):1297-305. doi: 10.1016/j.cellsig.2012.02.006. PubMed PMID: 22374304.
25. Detmar M, Orfanos CE. Tumor necrosis factor-alpha inhibits cell proliferation and induces class II antigens and cell adhesion molecules in cultured normal human keratinocytes in vitro. Archives of dermatological research. 1990;282(4):238-45. PubMed PMID: 2115318.
26. Hancock GE, Kaplan G, Cohn ZA. Keratinocyte growth regulation by the products of immune cells. The Journal of experimental medicine. 1988;168(4):1395-402. PubMed PMID: 2459297; PubMed Central PMCID: PMC2189076.
27. Saunders NA, Jetten AM. Control of growth regulatory and differentiation-specific genes in human epidermal keratinocytes by interferon gamma. Antagonism by retinoic acid and transforming growth factor beta 1. The Journal of biological chemistry. 1994;269(3):2016-22. PubMed PMID: 7904998.
28. Kono T, Tanii T, Furukawa M, Mizuno N, Taniguchi S, Ishii M, et al. Effects of human recombinant tumor necrosis factor-alpha (TNF-alpha) on the proliferative potential of human keratinocytes cultured in serum-free medium. The Journal of dermatology. 1990;17(7):409-13. PubMed PMID: 2229643.
29. Viard-Leveugle I, Gaide O, Jankovic D, Feldmeyer L, Kerl K, Pickard C, et al. TNF-alpha and IFN-gamma are potential inducers of Fas-mediated keratinocyte apoptosis through activation of inducible nitric oxide synthase in toxic epidermal necrolysis. The Journal of investigative dermatology. 2013;133(2):489-98. doi: 10.1038/jid.2012.330. PubMed PMID: 22992806.
30. Daehn IS, Varelias A, Rayner TE. T-lymphocyte-induced, Fas-mediated apoptosis is associated with early keratinocyte differentiation. Experimental dermatology. 2010;19(4):372-80. doi: 10.1111/j.1600-0625.2009.00917.x. PubMed PMID: 19645855.

31. Karim R, Meyers C, Backendorf C, Ludigs K, Offringa R, van Ommen GJ, et al. Human papillomavirus deregulates the response of a cellular network comprising of chemotactic and proinflammatory genes. PloS one. 2011;6(3):e17848. doi: 10.1371/journal.pone.0017848. PubMed PMID: 21423754; PubMed Central PMCID: PMC3056770.
32. McLaughlin-Drubin ME, Christensen ND, Meyers C. Propagation, infection, and neutralization of authentic HPV16 virus. Virology. 2004;322(2):213-9. doi: 10.1016/j.virol.2004.02.011. PubMed PMID: 15110519.
33. Meyers C, Mayer TJ, Ozbun MA. Synthesis of infectious human papillomavirus type 18 in differentiating epithelium transfected with viral DNA. Journal of virology. 1997;71(10):7381-6. PubMed PMID: 9311816; PubMed Central PMCID: PMC192083.
34. Jones LJ, Gray M, Yue ST, Haugland RP, Singer VL. Sensitive determination of cell number using the CyQUANT cell proliferation assay. Journal of immunological methods. 2001;254(1-2):85-98. PubMed PMID: 11406155.
35. Mulay SR, Desai J, Kumar SV, Eberhard JN, Thomasova D, Romoli S, et al. Cytotoxicity of crystals involves RIPK3-MLKL-mediated necroptosis. Nature communications. 2016;7:10274. doi: 10.1038/ncomms10274. PubMed PMID: 26817517; PubMed Central PMCID: PMC4738349.
36. Ohnishi S, Okabe K, Obata H, Otani K, Ishikane S, Ogino H, et al. Involvement of tazarotene-induced gene 1 in proliferation and differentiation of human adipose tissue-derived mesenchymal stem cells. Cell proliferation. 2009;42(3):309-16. doi: 10.1111/j.1365-2184.2008.00592.x. PubMed PMID: 19250291.
37. Wu CC, Tsai FM, Shyu RY, Tsai YM, Wang CH, Jiang SY. G protein-coupled receptor kinase 5 mediates Tazarotene-induced gene 1-induced growth suppression of human colon cancer cells. BMC cancer. 2011;11:175. doi: 10.1186/1471-2407-11-175. PubMed PMID: 21575264; PubMed Central PMCID: PMC3112162.
38. Han J, Zhong CQ, Zhang DW. Programmed necrosis: backup to and competitor with apoptosis in the immune system. Nature immunology. 2011;12(12):1143-9. doi: 10.1038/ni.2159. PubMed PMID: 22089220.
39. Wang L, Du F, Wang X. TNF-alpha induces two distinct caspase-8 activation pathways. Cell. 2008;133(4):693-703. doi: 10.1016/j.cell.2008.03.036. PubMed PMID: 18485876.
40. He S, Wang L, Miao L, Wang T, Du F, Zhao L, et al. Receptor interacting protein kinase-3 determines cellular necrotic response to TNF-alpha. Cell. 2009;137(6):1100-11. doi: 10.1016/j.cell.2009.05.021. PubMed PMID: 19524512.
41. Degterev A, Huang Z, Boyce M, Li Y, Jagtap P, Mizushima N, et al. Chemical inhibitor of nonapoptotic cell death with therapeutic potential for ischemic brain injury. Nature chemical biology. 2005;1(2):112-9. doi: 10.1038/nchembio711. PubMed PMID: 16408008.
42. Koo GB, Morgan MJ, Lee DG, Kim WJ, Yoon JH, Koo JS, et al. Methylation-dependent loss of RIP3 expression in cancer represses programmed necrosis in

response to chemotherapeutics. Cell research. 2015;25(6):707-25. doi: 10.1038/cr.2015.56. PubMed PMID: 25952668; PubMed Central PMCID: PMC4456623.
43. Hyland PL, McDade SS, McCloskey R, Dickson GJ, Arthur K, McCance DJ, et al. Evidence for alteration of EZH2, BMI1, and KDM6A and epigenetic reprogramming in human papillomavirus type 16 E6/E7-expressing keratinocytes. Journal of virology. 2011;85(21):10999-1006. doi: 10.1128/JVI.00160-11. PubMed PMID: 21865393; PubMed Central PMCID: PMC3194988.
44. Sun S, Yu F, Zhang L, Zhou X. EZH2, an on-off valve in signal network of tumor cells. Cellular signalling. 2016;28(5):481-7. doi: 10.1016/j.cellsig.2016.02.004. PubMed PMID: 26876615.
45. Tan J, Yang X, Zhuang L, Jiang X, Chen W, Lee PL, et al. Pharmacologic disruption of Polycomb-repressive complex 2-mediated gene repression selectively induces apoptosis in cancer cells. Genes & development. 2007;21(9):1050-63. doi: 10.1101/gad.1524107. PubMed PMID: 17437993; PubMed Central PMCID: PMC1855231.
46. Miranda TB, Cortez CC, Yoo CB, Liang G, Abe M, Kelly TK, et al. DZNep is a global histone methylation inhibitor that reactivates developmental genes not silenced by DNA methylation. Molecular cancer therapeutics. 2009;8(6):1579-88. doi: 10.1158/1535-7163.MCT-09-0013. PubMed PMID: 19509260; PubMed Central PMCID: PMC3186068.
47. Yang G, Xu Y, Chen X, Hu G. IFITM1 plays an essential role in the antiproliferative action of interferon-gamma. Oncogene. 2007;26(4):594-603. doi: 10.1038/sj.onc.1209807. PubMed PMID: 16847454.
48. Ackrill AM, Reid LE, Gilbert CS, Gewert DR, Porter AC, Lewin AR, et al. Differential response of the human 6-16 and 9-27 genes to alpha and gamma interferons. Nucleic acids research. 1991;19(3):591-8. PubMed PMID: 1901407; PubMed Central PMCID: PMC333653.
49. Friedman RL, Manly SP, McMahon M, Kerr IM, Stark GR. Transcriptional and posttranscriptional regulation of interferon-induced gene expression in human cells. Cell. 1984;38(3):745-55. PubMed PMID: 6548414.
50. Kelly JM, Gilbert CS, Stark GR, Kerr IM. Differential regulation of interferon-induced mRNAs and c-myc mRNA by alpha- and gamma-interferons. European journal of biochemistry / FEBS. 1985;153(2):367-71. PubMed PMID: 3935435.
51. Muller M, Laxton C, Briscoe J, Schindler C, Improta T, Darnell JE, Jr., et al. Complementation of a mutant cell line: central role of the 91 kDa polypeptide of ISGF3 in the interferon-alpha and -gamma signal transduction pathways. The EMBO journal. 1993;12(11):4221-8. PubMed PMID: 7693454; PubMed Central PMCID: PMC413716.
52. Fuentes-Gonzalez AM, Contreras-Paredes A, Manzo-Merino J, Lizano M. The modulation of apoptosis by oncogenic viruses. Virology journal. 2013;10:182. doi: 10.1186/1743-422X-10-182. PubMed PMID: 23741982; PubMed Central PMCID: PMC3691765.

53. Hamid NA, Brown C, Gaston K. The regulation of cell proliferation by the papillomavirus early proteins. Cellular and molecular life sciences : CMLS. 2009;66(10):1700-17. doi: 10.1007/s00018-009-8631-7. PubMed PMID: 19183849.
54. Mocarski ES, Upton JW, Kaiser WJ. Viral infection and the evolution of caspase 8-regulated apoptotic and necrotic death pathways. Nature reviews Immunology. 2012;12(2):79-88. doi: 10.1038/nri3131. PubMed PMID: 22193709; PubMed Central PMCID: PMC4515451.
55. Cho YS, Challa S, Moquin D, Genga R, Ray TD, Guildford M, et al. Phosphorylation-driven assembly of the RIP1-RIP3 complex regulates programmed necrosis and virus-induced inflammation. Cell. 2009;137(6):1112-23. doi: 10.1016/j.cell.2009.05.037. PubMed PMID: 19524513; PubMed Central PMCID: PMC2727676.
56. Huang Z, Wu SQ, Liang Y, Zhou X, Chen W, Li L, et al. RIP1/RIP3 binding to HSV-1 ICP6 initiates necroptosis to restrict virus propagation in mice. Cell host & microbe. 2015;17(2):229-42. doi: 10.1016/j.chom.2015.01.002. PubMed PMID: 25674982.
57. Upton JW, Kaiser WJ, Mocarski ES. Virus inhibition of RIP3-dependent necrosis. Cell host & microbe. 2010;7(4):302-13. doi: 10.1016/j.chom.2010.03.006. PubMed PMID: 20413098; PubMed Central PMCID: PMC4279434.
58. Bhanja Chowdhury J, Shrivastava S, Steele R, Di Bisceglie AM, Ray R, Ray RB. Hepatitis C virus infection modulates expression of interferon stimulatory gene IFITM1 by upregulating miR-130A. Journal of virology. 2012;86(18):10221-5. doi: 10.1128/JVI.00882-12. PubMed PMID: 22787204; PubMed Central PMCID: PMC3446586.
59. Wee ZN, Li Z, Lee PL, Lee ST, Lim YP, Yu Q. EZH2-mediated inactivation of IFN-gamma-JAK-STAT1 signaling is an effective therapeutic target in MYC-driven prostate cancer. Cell reports. 2014;8(1):204-16. doi: 10.1016/j.celrep.2014.05.045. PubMed PMID: 24953652.
60. Zhang L, Wu J, Ling MT, Zhao L, Zhao KN. The role of the PI3K/Akt/mTOR signalling pathway in human cancers induced by infection with human papillomaviruses. Molecular cancer. 2015;14:87. doi: 10.1186/s12943-015-0361-x. PubMed PMID: 26022660; PubMed Central PMCID: PMC4498560.

SUPPLEMENTARY INFORMATION

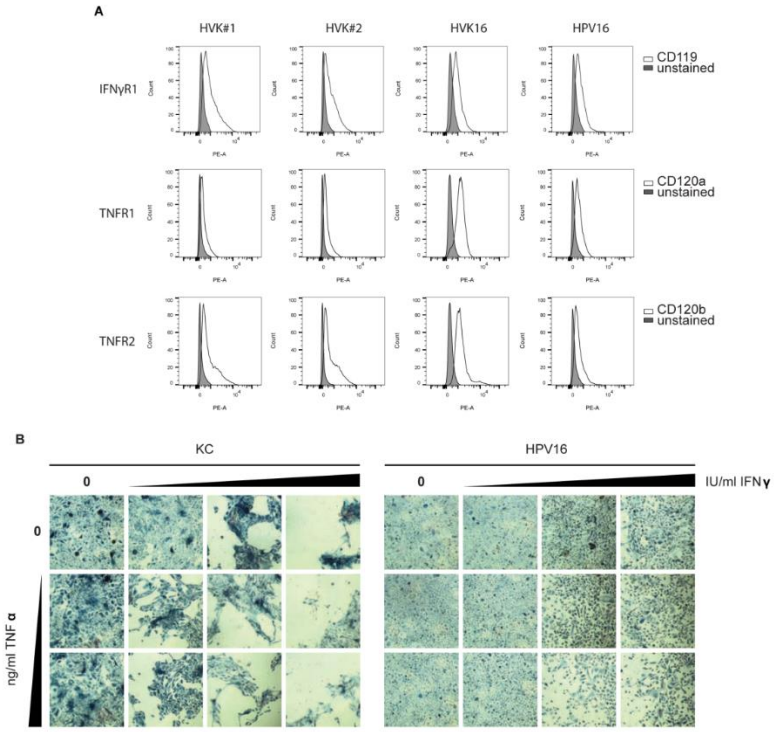

Supplemental Figure 1. The different effect of IFNγ and TNFα on HPV+ KCs is not due to alterations in cell surface expression of the receptors. (A) Cell surface expression of IFNγR1 (CD119), TNFR1 (CD120a) and TNFR2 (CD120b) of the indicated cell lines was analyzed by flow cytometry using phycoerythrin-conjugated antibodies. (B) Undifferentiated KCs (HFK) and HPV16+KCs (HPV16) were treated with increasing doses of IFNγ and/or TNFα for 72 hours after which cell confluency was monitored by MTT staining and phase-contrast microscopy as a measure for proliferation [60]. Representative microscopy pictures (4x magnification) are shown.

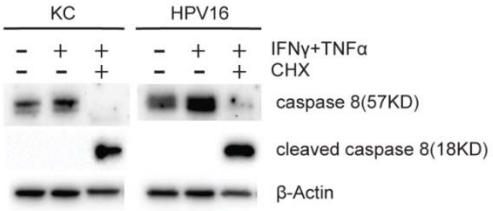

Supplemental Figure 2. Fully cleaved caspase-8 requires co-treatment of KCs with cycloheximide. Caspase-8 (57 kD) and fully cleaved caspase-8 (18 kD) protein level in KC and HPV16+KC stimulated with/without 50 IU/ml IFNγ, 30 ng/ml TNFα, and 100 μg/ml cycloheximide (CHX) for 48 hours, as measured by WB. ⊠-actin served as loading control.

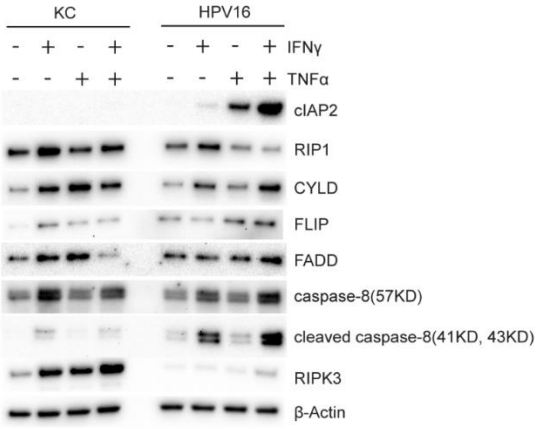

Supplemental Figure 3. The expression of RIPK3 is enhanced by both IFNγ and TNFα.
The KC and HPV16+KCs were stimulated with 50 IU/ml IFNγ and/or 30 ng/ml TNFα for 24 hours. The protein expression levels of cIAP2, RIP1, CYLD, FLIP, FADD, caspase-8 (57 kD), cleaved caspase-8 (41 kD, 43 kD), and RIPK3 was measured by western blotting (WB) in whole cell extracts. β-actin served as loading control.

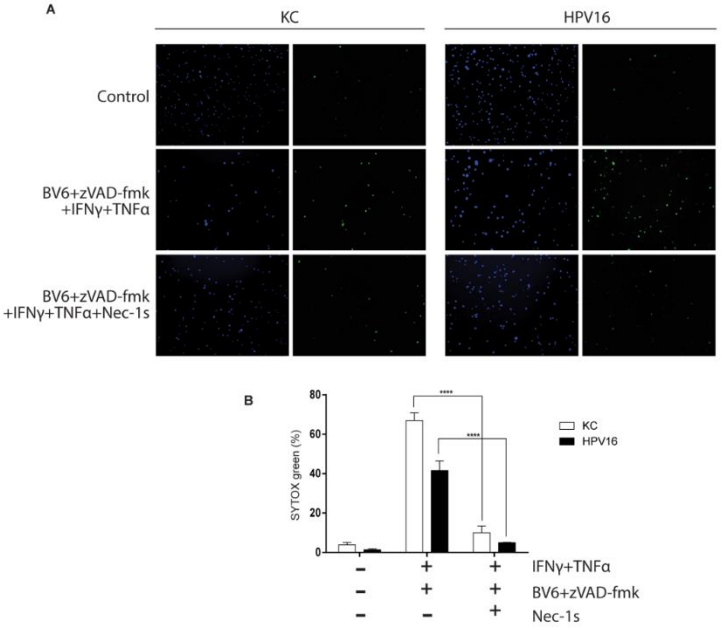

Supplemental Figure 4. The induction of IFNγ and TNFα-induced necroptosis is prevented by co-treatment with necrostatin-1s.
(A) Undifferentiated KCs (HVK#1)_and HPV16+KC (HPV16) were treated with or without 250 IU/ml IFNγ, 250 ng/ml TNFα, 5 μM BV6, 20 μM zVAD-fmk and/or 20 μM necrostatin-1s (Nec-1s) as indicated, for 48 hours. All cell nuclei were labelled with DAPI (blue fluorescence). Dead cells were stained using SYTOX green dead cell stain resulting in green fluorescent nuclei of dead cells.
(B) The number of dead cells among all cells was counted in multiple fields. The percentage of cell death was calculated. ****P < 0.001.

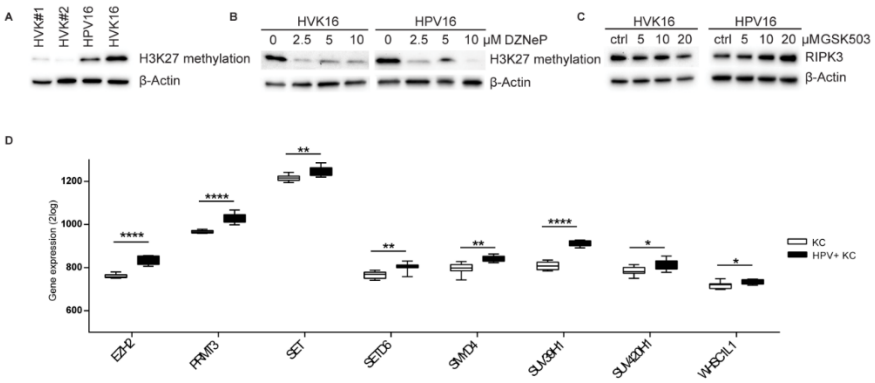

E

ASH1L	MLL5	SETD2	SMYD1	WHSC1L1
C5orf35	NSD1	SETD3	SMYD2	
DOT1L	NSD1	SETD4	SMYD3	
EHMT1	PRDM2	SETD5	SMYD4	
EHMT2	PRMT3	SETD6	SMYD5	
EZH1	PRDM9	SETD7	SUV39H1	
EZH2	SET	SETD8	SUV39H2	
MLL	SETBP1	SETDB1	SUV420H1	
MLL2	SETD1A	SETDB2	SUV420H2	
MLL3	SETD1B	SETMAR	WHSC1	

Supplemental Figure 5. Methylation of H3K27 in KCs and HPV16+ KCs and catalytic inhibition of EZH2 and expression of methyltransferases
(A) H3K27 methylation in KCs and HPV16+ KCs.
(B) The protein expression levels of H3K27 methylation were analysed in the two independent HPV16+KCs (HVK16, HPV16) either 72 hours after treatment with DZNeP.
(C) The protein expression levels of RIPK3 were analysed in the two independent HPV16+KCs (HVK16, HPV16) either 72 hours after treatment with GSK503, the catalytic inhibitor of EZH2, at indicated concentrations.
(D) Microarray gene expression values for methyltransferases significantly different expressed between 4 independent uninfected KCs and 4 independent hrHPV+KCs, represented in a box plot. * p<0.05.
(E) List of methyltransferases analyzed in microarray.

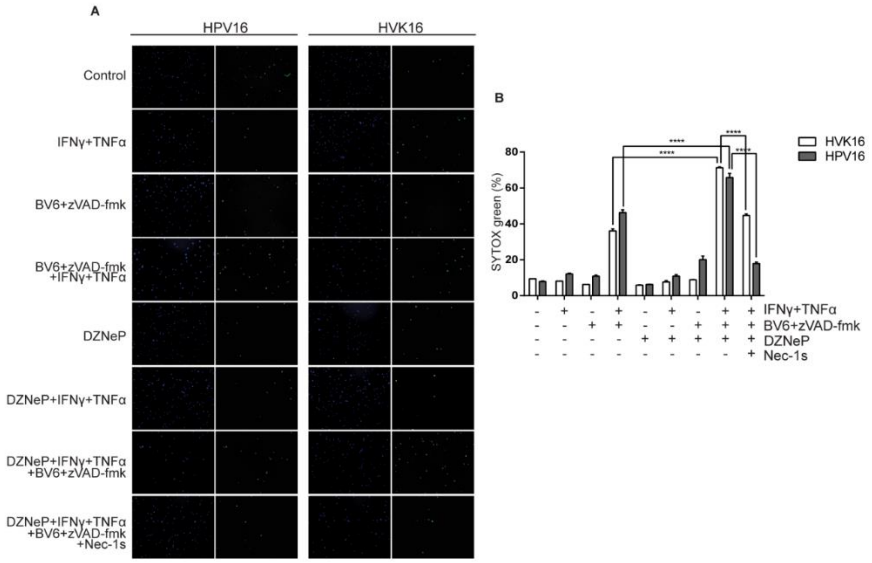

Supplemental Figure 6. Blocking global histone methylation rescues the induction of necroptosis by IFNγ and TNFα.
(A,B) The two HPV16+KCs (HVK16, HPV16) were treated with or without 10 μM DZNeP. After 24 hours, the cells were treated with 250 IU/ml IFN γ, 250 ng/ml TNFα, 5 μM BV6, 20 μM zVAD-fmk and/or 20 μM Nec-1s as indicated for 48 hours. All cell nuclei were labelled with DAPI (blue fluorescence). Dead cells were stained using SYTOX green dead cell stain resulting in green fluorescent nuclei of dead cells. (A) Representative example. (B) The percentage of cell death measured for each treatment was plotted for both HPV16+KC cultures. ****P < 0.001.

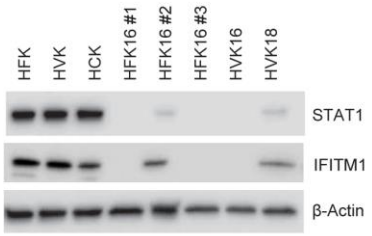

Supplemental Figure 7. Expression of STAT1 and IFITM1 in uninfected and hrHPV+ KCs.
STAT1 and IFITM1 protein levels in 3 independent KC, 4 independent HPV16+KC, and 1 HPV18+KC cultures as measured by western blotting (WB) in whole cell extracts. ⊠-actin served as loading control.

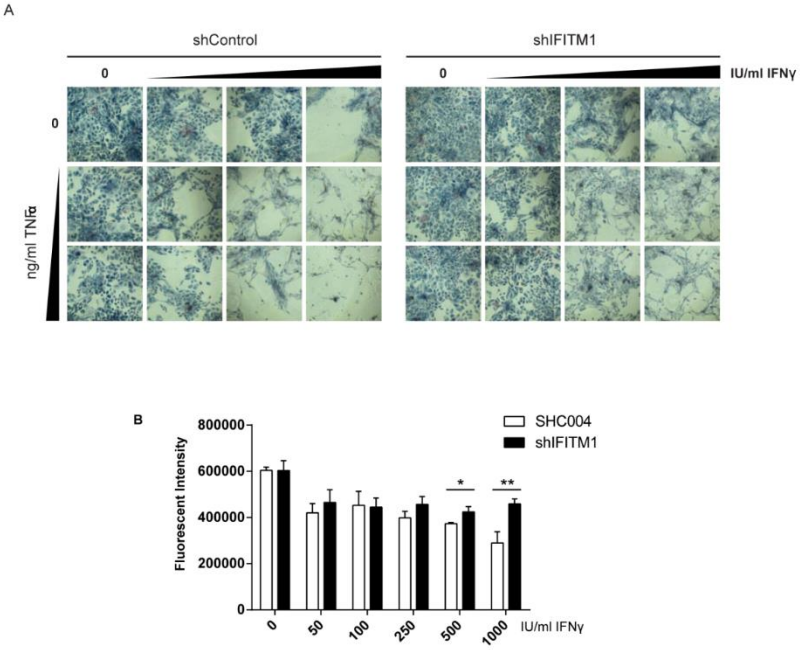

Supplemental Figure 8. Increased capacity of normal keratinocytes to resist IFNγ and TNFα-induced growth arrest after knock-down of IFITM1.
(A) Control and IFITM1 knock-down undifferentiated uninfected KCs were treated with IFNγ and/or TNFα for 96 hours after which cell confluency was monitored by MTT staining and phase-contrast microscopy as a measure for proliferation. Representative microscopy pictures (4x magnification) are shown.
(B) Control and IFITM1 knock-down undifferentiated uninfected KCs were treated with indicated doses of IFNγ for 96 hours after which the cellular DNA contents, as a measure of cell proliferation, was quantified using the CyQuant-NF assay. Knock-down of IFITM1 results in significant resistance to IFNγ mediated control of proliferation at the higher doses of IFNγ used.